

A K-band Resonant Impedance Tuner with a Solid-State Hybrid Tuning

Mohammad Abu Khater, Muna Awajan, and Dimitrios Peroulis

School of Electrical and Computer Engineering Purdue University

West Lafayette, IN, USA (mabukhater@ieee.org)

Abstract—This paper presents the first K-band resonant impedance tuner based on a solid-state hybrid tuning system. The tuner employs two coupled high-inductance resonators controlled by a hybrid combination of PIN diodes and varactor diodes. The high-inductance resonator design is key to minimizing the effect of the tuning elements on the quality factor of the resonators. Employing solid-state tuning elements is critical for maintaining fast tuning speed. The presented design is experimentally validated with a proof-of-concept demonstration in the 23–25 GHz range with 576 impedance points per frequency and a tuning time of 100 ns. To the authors' best knowledge, this is the first high-*Q* stand-alone solid-state mmWave impedance tuner.

Index Terms—Impedance tuner, solid-state switches, evanescent-mode resonators, tuning speed.

I. INTRODUCTION

Impedance tuners are critical components for numerous applications including device characterization, adaptive load matching, and stability testing. The accompanying performance measures often include impedance range, loss, and tuning speed. Several methods and technologies have been explored to build high-frequency impedance tuners. Impedance tuners that rely on solid-state devices provide fast tuning speed and a reasonable coverage of the Smith chart. These are typically varactor-based [1], [2], or switch-based [3] devices. The finite resistance of the solid-state devices, however, limits their useful range to just few GHz [4]. Alternatively, MEMS-based tuners have shown low loss and high impedance tuning range at millimeter-wave (mmWave) frequencies [5]–[7]. MEMS mmWave devices, however, are typically limited to cold-switching, and they are also not readily available as low-cost integrable components.

This paper presents a unique approach that, for the first time, enables the implementation of high-quality K-band impedance tuners with just commercially-available solid-state tuning devices. Unlike conventional approaches, our proposed method relies on loading high-inductance high-*Q* resonators with switched capacitors as shown schematically in Fig. 1(a). Compared to conventional distributed impedance tuners in [1]–[3], [5]–[7], the resonator-based ones allow for minimizing the effect of the switching device on the overall tuner loss. This can be concluded from the quality factor of the series RC circuit formed by the capacitors and the switches ($Q = 1/(\omega R_S C_S)$, R_S : switch ON resistance, C_S : switched capacitance). For a constant R_S , the quality factor can be increased by reducing the C_S , while the resonant frequency is adjusted in the design using the equivalent inductance of

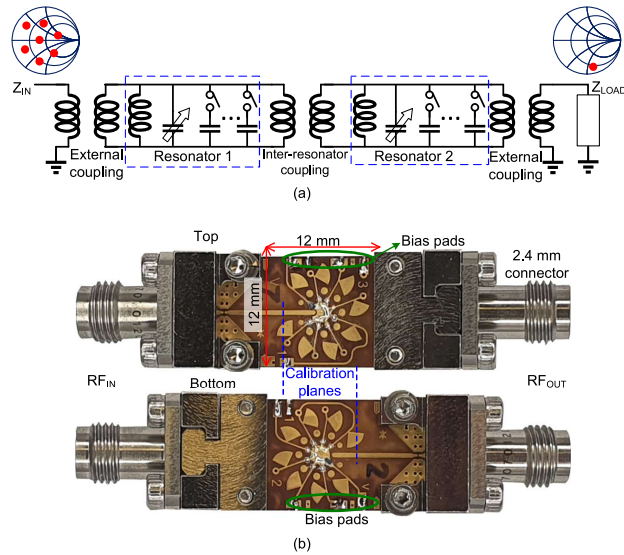


Fig. 1. (a) The presented impedance tuner utilizes high-inductance, high-*Q* resonators loaded with a hybrid tuning system of switched capacitors and varactors. The capacitors are switched such that the resonant frequencies are independently tuned, resulting in various impedances at the input. (b) The implemented resonator-based impedance tuner prototype for validating the proposed concept.

the resonator. The hybrid tuning scheme implemented by employing both switched capacitors and varactor diodes is an additional innovation of the proposed design. This allows for both coarse- and fine-tuning of the desired impedance range.

We experimentally validate the proposed impedance tuner concept by implementing a proof-of-concept prototype in the 23–25 GHz frequency range using a commercial PCB fabrication process as shown in Fig. 1(b). To the best of the authors' knowledge, this demonstration is the only successful tuner above S band with solid-state tuning elements that exhibits a reasonable impedance coverage with 100 ns tuning time.

II. IMPEDANCE TUNER DESIGN

A. Structure

A simplified cross section of the presented impedance tuner is shown in Fig. 2(a). Two high-*Q* evanescent-mode resonators [8], [9] are stacked vertically, with an opening between them on Layer 3 to realize the inter-resonator coupling. The external coupling is realized with tapping vias from Layer 1/5 to Layer 3.

The resonators are defined with plated vias between Layers 2 and 3. The same applies to the loading post. The vias are shown in Fig. 2(b). Both resonators have a similar structure.

To tune the resonant frequency, PIN diodes are used to switch the capacitive pads. A total of seven PIN diodes are used in three binary-weighted groups (1+2+4). An eighth capacitive pad is used with a varactor for fine-tuning. The order of the PIN diodes and the location of the varactor are shown in Fig. 2(c).

When any of the PIN diodes is ON, the loading impedance of the resonator becomes a series RC circuit formed by the resistance of the diodes ($\sim 4 \Omega$ for DSM8100), and the capacitance of the pads (75 fF). For the OFF case, the resistance is replaced with the OFF capacitance of the PIN diode (~ 15 fF). This results in a $C_{ON}/C_{OFF} = 75/12.5$. The varactors (MAVR-011020-14110P) are also connected to a capacitive pad, and result in a capacitance range of 26–50 fF. These relatively low capacitance values increase the quality factor of the resonators as discussed in the introduction. The resonators are then designed such that they tune around the design center frequency of 24 GHz.

B. Bias Decoupling

In order to properly bias the diodes, radial stubs are used as shown in Fig. 2(c). Single-sided stubs are used to reduce the required area. Compared to double-sided stubs, however, no noticeable difference in performance exists.

At the pointing tip of the stub, a low-impedance node is created. In addition, the length of the line connecting the radial stub with the capacitive pads is $\lambda/4$ at 24 GHz. As a result, the impedance seen from the capacitive pads side is sufficiently high. Consequently, the switched impedance is dominated by the capacitive pads. In other words, the bias decoupling delivers the dc bias, without affecting the ac performance.

III. FABRICATION AND MEASUREMENTS

The impedance tuner stackup, shown in Fig. 2, is built using Astra MT77 substrates. The thicknesses are 0.2 mm for the top and bottom substrates, and 0.5 mm for the middle substrates. The assembled PCB is shown in Fig. 1(b). The tuner occupies an area of 12 mm \times 12 mm. Two 2.4-mm connectors are used for testing. Fig. 1(b) also shows the necessary bias traces used to carry the dc voltages to the PIN and the varactor diodes.

The impedance tuner has 64 switching states (2^6). For each state, the varactor voltages are set to 2, 6, and 10 V. As a result, the total number of measured points is 576 for each frequency. Additional points may be generated by applying different bias voltages. The impedance coverage, however, is not expected to be affected significantly.

The impedance tuner operates in the continuous frequency range 23–25 GHz, which includes part of the newly adopted 5G bands. The simulated and measured Smith chart coverages are shown in Fig. 3. The quantity ($|S_{11}|^2 + |S_{21}|^2$) is also plotted in the color map as a measure of loss. The losses are dominated by the equivalent resistances of the diodes. This is verified in simulations. The measured maximum reflection

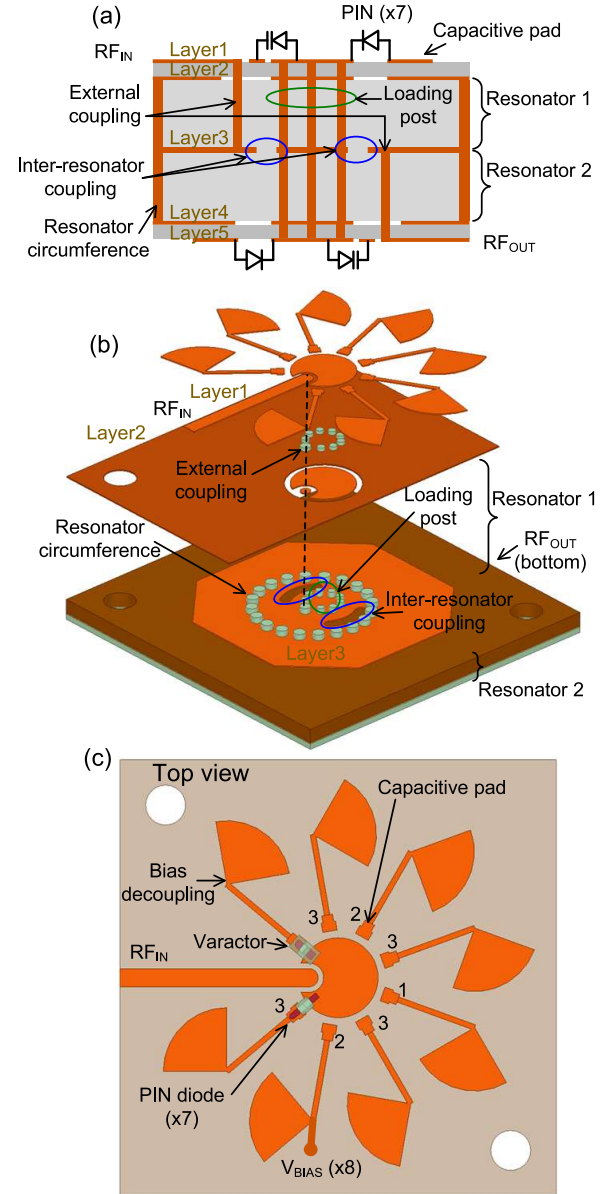


Fig. 2. (a) A cross section of the impedance tuner in a 5-layer PCB structure. The evanescent-mode structure is formed by the outer vias (shown as the resonator circumference) and the post vias in the middle. The PIN diodes, and varactors for fine-tuning, are placed on the top and bottom layers. (b) A 3D exploded view of the impedance tuner. One resonator is shown in the schematic. Both resonators have a similar structure. (c) The top view of the impedance tuner showing an example of the placement of the diodes. Radial stubs provide high impedances at the capacitive pads for proper biasing.

(Γ_{max}) is around 0.94 for all frequencies. The differences between the measurements and simulations are due to fabrication tolerances and the manual assembly process. For example, measurements show that a 1-mil variation in the board thickness cause approximately 50% reduction in Smith chart coverage.

Compared to impedance tuners based on MEMS technologies, this tuner has a significantly faster response time. Response time is critical if the impedance tuner is intended to

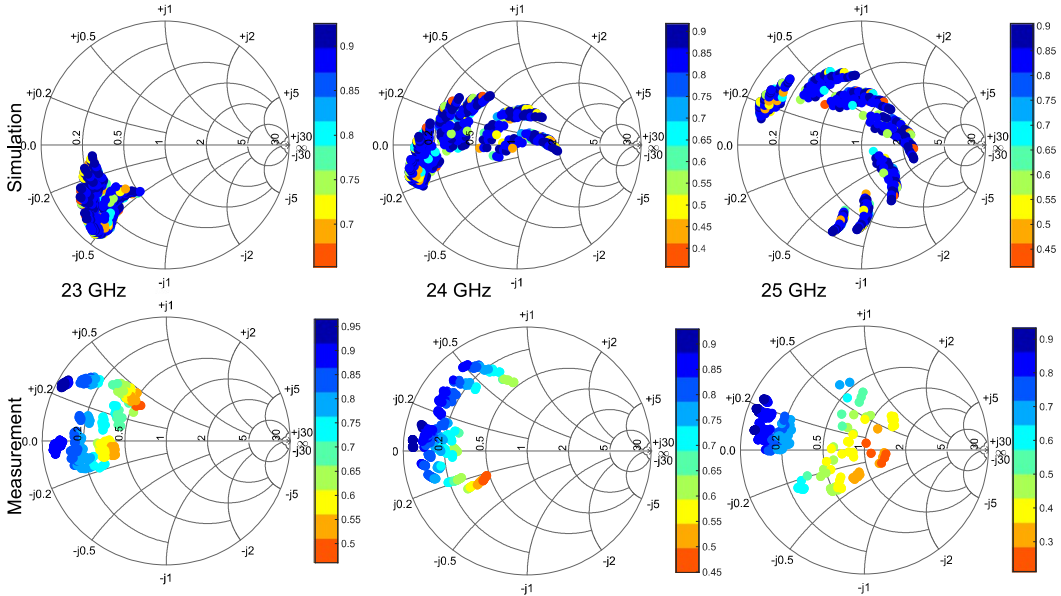


Fig. 3. Simulated (top) and measured (bottom) Smith chart coverage of the impedance tuner. The color map in each Smith chart quantifies the value of $|S_{11}|^2 + |S_{21}|^2$.

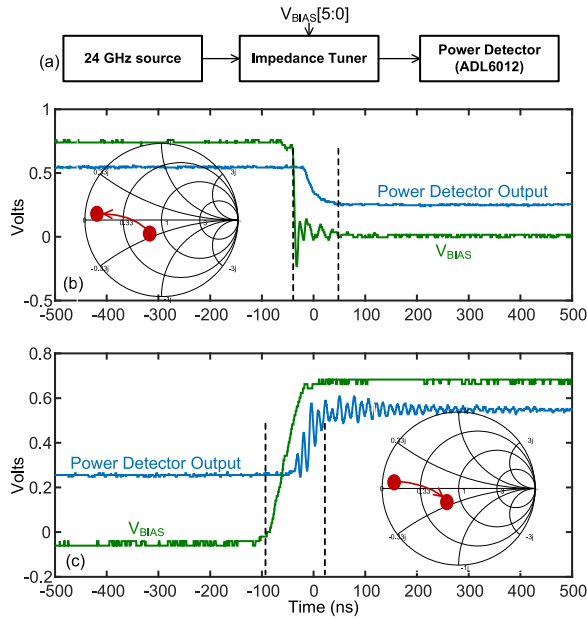


Fig. 4. (a) The measurement setup for the response time. (b) The time-domain output power from the impedance tuner when switching from a low-reflection impedance to a high-reflection impedance. (c) The time-domain output power from the impedance tuner when switching from a high-reflection impedance to a low-reflection impedance.

be used in real-time adaptive front-ends. The response time is measured by switching between a high-reflection and a low-reflection impedance, and then measuring the output power with a wideband power detector (ADL6012). This setup is shown in Fig. 4(a).

The results in Fig. 4(b) and (c), taken at 24 GHz, show that the impedance tuner can settle between the two switched

TABLE I
COMPARISON WITH STATE-OF-THE-ART.

Ref.	Technology	Frequency (GHz)	Impedance points	Tuning time
[5]	MEMS	20–50	256	100's μ s*
[6]	MEMS	30	Continuous	100's μ s*
[7]	MEMS	6	Continuous	10's ms*
[3]	Solid-State	1.7–2.6	1024	100's ns*
[2]	Solid-State	2.14	Continuous	100's ns*
[1]	Solid-State	2–3	Continuous	100's ns*
This work	Solid-State	23–25	576	100 ns

*: Estimated from technology

impedances within ~ 100 ns. The ringing observed in Fig. 4(c) is attributed to the biasing circuit. This is significantly faster than MEMS-based tuners, with a minimal penalty on loss.

Table I summarizes the comparison with the state-of-the-art. The presented impedance tuner shows the highest operating frequency of solid-state tuner. In addition, it has the fastest response time among mmWave tuners.

IV. CONCLUSION

This paper presented the first K-band impedance tuner based on a solid-state hybrid tuning. The design is optimized to reduce the effect of the finite resistance of the tuning diodes by employing a novel architecture of high-inductance high-quality resonators. The experimentally demonstrated tuner significantly extends the operating frequency range compared to state-of-the-art solid-state tuners. In addition, it shows the fastest response time of 100 ns compared to mmWave tuners. This performance is suitable for adaptive 5G front-end applications.

REFERENCES

- [1] K. W. Wong and R. R. Mansour, "Impedance tuner using bst varactors in alumina-based ipd technology," in *2016 46th European Microwave Conference (EuMC)*, 2016, pp. 1051–1054.
- [2] S. Jeong, J. Jeong, and Y. Jeong, "A design of a impedance tuner with programmable characteristic for rf amplifiers," *IEEE Microwave and Wireless Components Letters*, vol. 27, no. 5, pp. 473–475, 2017.
- [3] A. Y.-S. Jou, C. Liu, and S. Mohammadi, "An integrated reconfigurable tuner in 45nm CMOS SOI technology," in *IEEE Topical Meeting on Silicon Monolithic Integrated Circuits in RF Systems*, 2015, pp. 67–69.
- [4] M. Abu Khater, K. Zeng, and D. Peroulis, "Temperature-compensated lumped element tunable bandpass filter," in *2016 IEEE MTT-S International Microwave Symposium (IMS)*, 2016, pp. 1–4.
- [5] T. Vaha-Heikkila and G. Rebeiz, "A 20-50 ghz reconfigurable matching network for power amplifier applications," in *IEEE MTT-S International Microwave Symposium Digest*, vol. 2, 2004, pp. 717–720 Vol.2.
- [6] Y. Lu, L. Katehi, and D. Peroulis, "A novel MEMS impedance tuner simultaneously optimized for maximum impedance range and power handling," in *IEEE International Microwave Symp.*, 2005, pp. 927–930.
- [7] T. Singh, N. K. Khaira, and R. R. Mansour, "Monolithically integrated reconfigurable RF MEMS based impedance tuner on SOI substrate," in *IEEE MTT-S International Microwave Symposium*, 2019, pp. 790–792.
- [8] M. Abu Khater, Y. Wu, and D. Peroulis, "Tunable cavity-based diplexer with spectrum-aware automatic tuning," *IEEE Transactions on Microwave Theory and Techniques*, vol. 65, no. 3, pp. 934–944, 2017.
- [9] M. Abu Khater and D. Peroulis, "Dual-band dual-mode filter-enhanced linearity measurement," *IEEE Microw. Wireless Compon. Lett.*, vol. 31, no. 9, pp. 1083–1085, 2021.